SYNTHESIS, CRYSTAL STRUCTURE AND OPTICAL PROPERTIES OF N,N′-DIMETHYLFORMAMIDE ADDUCT OF TETRAKIS(THIOCYANATO)MANGANESE(II)MERCURY(II) COMPLEX

[1]* S. Parthiban, [2] Subbiah Meenakshisundaram

[1]Assistant Professor, [2] Emeritus Professor
[1,2] Department of Chemistry
[1,2] Annamalai University, Annamalainagar 608 002, Tamilnadu, India

***ABSTRACT:** The crystal structure of $MnHg(SCN)_4(L)$ (L=DMF) (MMTDMF) has been determined by X-ray crystallography and refined to conventional R value of 0.0395 (final R indices). The crystal system is monoclinic with space group P21/c and the unit cell contains four molecules (Z=4). Ambidentate SCN^- ion acts as a bridging ligand connecting the distorted tetrahedron and octahedron. N,N′-Dimethylformamide (DMF) is coordinated to manganese atom through O(DMF) atom. Comparative analysis made with $MnHg(SCN)_4$ (MMTC) revealed that the high nonlinearity of MMTC is not facilitated by the coordination of MMTC with DMF and the MMTDMF polymer is centrosymmetric leading to NLO inactivity. The results are rationalized by correlating the NLO properties with structure.*

***Keywords** - coordination polymer, X-ray structure.*

---

1. INTRODUCTION

Nonlinear optical materials have wide applications including telecommunications, optical computing, information processing, data storage, laser remote sensing, color displays and medical diagnostics [1]. The organometallic complexes and their Lewis base adducts are generally good NLO materials [2]. In these semiorganic crystals relatively strong metal-ligand bond gives good stability and high nonlinearity [3], sharing the advantages of both organic and inorganic crystals. Further, the charge transfer transitions from metal to ligand (MLCT) or ligand to metal (LMCT) lead to high SHG conversion efficiency, most intensively studied NLO phenomenon.

It has been previously reported that the structural modifications of the counter anion of 4-N,N-dimethylamino-4′-N′-methylstilbazolium tosylate (DAST) considerably affect the crystal structure and NLO activity of stilbazolium derivatives [4]. In the present investigations, we have tried to correlate the NLO property with structure using the well known and highly efficient NLO material $MnHg(SCN)_4$ (MMTC) [5, 6] and its coordination polymer $MnHg(SCN)_4(C_3H_7NO)$ (MMTDMF). In this paper we report the structure, optical properties, morphology and SHG of MMTDMF.

2. EXPERIMENTAL

2.1. Synthesis and crystal growth

The synthesis of manganese mercury thiocyanate [7] was carefully done by stoichiometric incorporation of ammonium thiocyanate (Merck), manganese chloride (sd fine) and mercuric chloride (E. Merck) taken in the ratio of 4:1:1 respectively according to following chemical reaction:

$$4NH_4SCN + MnCl_2 + HgCl_2 \rightarrow \underset{(MMTC)}{MnHg(SCN)_4} + 4NH_4Cl$$

$$\underset{(MMTC)}{MnHg(SCN)_4} + \underset{(DMF)}{HCON(CH_3)_2} \rightarrow \underset{(MMTDMF)}{MnHg(SCN)_4(C_3H_7NO)}$$

The resulting greenish white MMTDMF was purified by repeated recrystallization. Seed crystals of MMTDMF were obtained by slow evaporation solution growth (SEST) technique. Compared to MMTC, MMTDMF is easily grown into large single crystals. Within 7–10 days, large number of tiny crystals with greenish white colour was formed by spontaneous nucleation. Best quality and highly transparent seed crystals are used in the preparation of bulk crystals. The grown crystals were harvested from aqueous growth medium after attaining a reasonable size. Figure 1 shows the as-grown bulk crystals of MMTDMF, with the dimensions of the 20×15×10 mm^3 and MMTC.

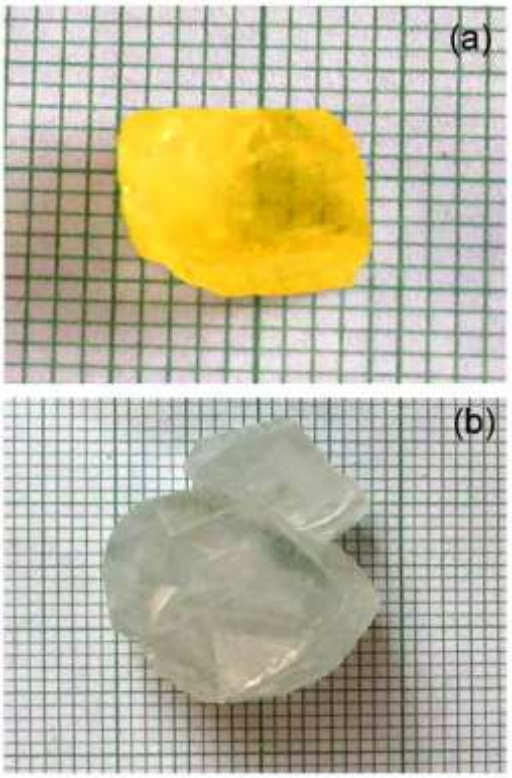

Fig. 1 Photographs of (a) MMTC crystal and (b) MMTDMF crystal

2.2. Characterization

The FT-IR spectra were recorded using AVATAR 330 FT-IR by KBr pellet technique. The XRD was performed by using Philips Xpert Pro Triple-axis X-ray diffractometer. Morphologies of the samples were observed by using JEOL JSM 5610 LV scanning electron microscope (SEM). The UV-Visible absorption spectra were recorded using Hitachi UV-Vis spectrophotometer in the spectral range 250–800 nm for all the samples. The Kurtz powder SHG instrument [8] was used for testing SHG. The structures were solved and refined by full matrix least squares on F^2 with Wingx software package utilizing SHELXS 97 and SHELXL 97 modules. The plots for the structures were created with DIAMOND software. Single crystal XRD data were collected on a diffraction system, which employs graphite monochromated MoKα radiation (λ = 0.71073 Å). All non-hydrogen atoms were refined anisotropically.

3. RESULTS AND DISCUSSION

3.1. FT-IR

It is well known that ν_{CN} stretching vibration often lies above 2100 cm^{-1}, the ν_{CS} stretching vibration lies between 860–780 cm^{-1} (N-bonding) or 720–690 cm^{-1} (S-bonding) and SCN bending vibration lies near 480 cm^{-1} (N-bonding) or 420 cm^{-1} (S-bonding) [9, 10].

The FT-IR spectrum of MMTDMF/KBr shows unique strong peak of C≡N at ~2138 cm^{-1} (Fig. 2). The CN stretching of NH_4CN is shifted from 2075 to ~2138 cm^{-1} in MMTDMF. Decrease of δ_{NCS} bending and ν_{CS} stretching in the coordination polymer compared with the corresponding bands in the free thiocyanate of NH_4SCN clearly confirm the metal-nitrogen and metal-sulfur coordination in their structures [2].

The weak absorption bands observed at ~897 and ~730 cm^{-1} are attributed to CS stretching of N-bonded and S-bonded complexes respectively. The deformation (SCN bending) vibration observed at ~471 cm^{-1} and a very weak band at ~416 cm^{-1} support the N-bonded and S-bonded nature of the complexes. In contrast, the IR of MMTC shows that ν_{CS} is shifted to higher frequencies. The broad band between 3500–3000 cm^{-1} corresponds to H_2O stretching. DMF shows a lower C=O stretching frequency at 1675 cm^{-1} than an unsubstituted C=O bond [11]. The IR spectrum of MMTDMF crystal is characterized by a very strong band in the region ~1650 cm^{-1} for the absorption of C=O which very much suggests that DMF has coordinated with MMTC through O(DMF). The position of the band is shifted upon coordination to metal ion. This value is close to the value previously observed for coordinated DMF in rhenium(IV) mononuclear compound [12]. The stretching and bending vibrations of metal ion centers always appear in the low frequency region [1]. The vibrational frequencies of the bridging coordination of SCN^- *i.e.,* M–SCN–M lie in the region 2180–2130 cm^{-1} (ν_{CN}) and 800–700 cm^{-1} (ν_{CS}) [13].

3.2. Powder XRD analysis

Powder XRD was performed at room temperature using a CuKα radiation of wavelength of 1.54 Å and covering diffraction angle 2θ from 20° to 90° with a step size of 0.008°. MMTC belongs to the tetragonal system [14] with the space group I4 while MMTDMF crystal belongs to monoclinic system with the space group $P2_1/c$. The X-ray powder diffraction experiment showed that the synthesized material MMTDMF contains a single phase (Fig. 3). The XRPD data for MMTDMF are listed in Table 1.

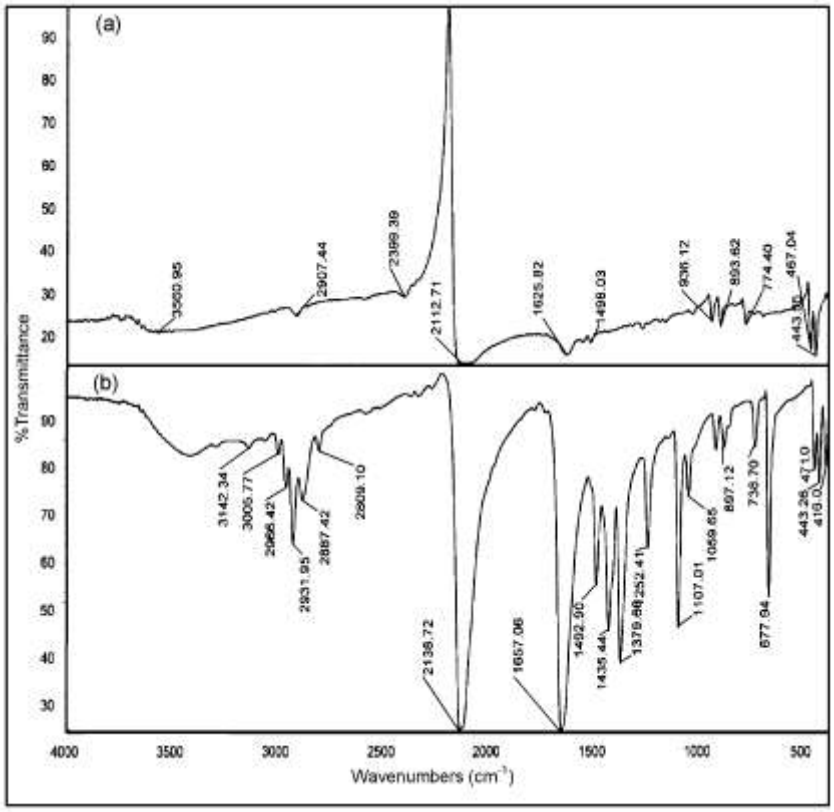

Fig. 2 FT-IR spectra of (a) MMTC and (b) MMTDMF

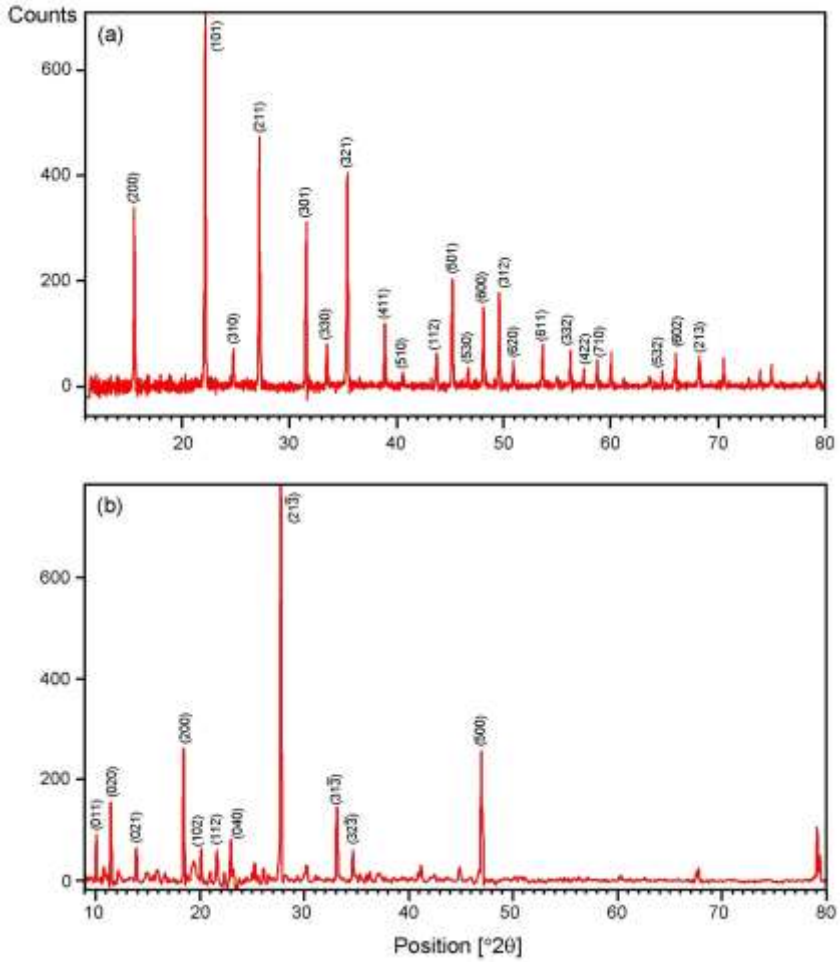

Fig. 3 XRD patterns of (a) MMTC and (b) MMTDMF

Table 1 The XRPD data for MMTDMF

h k l	Position [°2 Theta]	d-Spacing [Å]	Int. I/I_0 [%]
0 1 1	10.1284	8.73366	9.72
1 1 0	10.7976	8.19381	3.36
0 2 0	11.4171	7.75060	9.23

1 1-1	12.1999	7.25495	2.65
0 2 1	13.8724	6.38382	6.88
1 1 1	14.9545	5.92424	2.09
1 2-1	15.9238	5.56574	2.70
2 0 0	18.4497	4.80905	34.05
1 3 0	19.4720	4.55882	4.68
1 0 2	20.0777	4.42265	7.23
2 2-1	20.9769	4.23505	2.34
1 1 2	21.5858	4.11695	7.21
0 4 0	22.9469	3.87573	10.48
2 3 0	25.2201	3.53131	4.68
0 1 3	25.5555	3.48572	1.55
1 4 1	26.0900	3.41551	3.51
2 1-3	27.7537	3.21444	100.00
3 2-2	30.2255	2.95696	4.01
1 4 2	31.1964	2.86711	0.62
3 1-3	33.1118	2.70551	18.91
3 2-3	34.5992	2.59254	7.33
0 2 4	35.3341	2.54028	1.58
1 6 0	35.9285	2.49960	1.64
1 4 3	36.9531	2.43262	1.64
4 3 0	41.2707	2.18756	3.37
2 0 4	42.3213	2.13565	0.71
0 2 5	43.7744	2.06807	0.48
3 6 0	44.9041	2.01864	3.18
2 3 4	45.9312	1.97586	0.86
5 0 0	46.9277	1.93620	25.98
3 4-5	50.7226	1.79989	0.45
6 1 1	60.3155	1.53456	0.92
3 9-4	67.6582	1.38479	1.67
6 7-5	79.1399	1.21022	12.61

3.3. Single crystal XRD analysis and crystal structure of $MnHg(SCN)_4(C_3H_7NO)$

Thiocyante ion is a typical ambidentate ligand involving two different terminal donor atoms, the soft donor 'S' atom and 'hard' donor 'N' atom [15]. The molecular structure for MMTDMF was determined by single crystal X-ray diffraction analysis. The molecular structure and atom labeling scheme and projections of the stacking structure are shown in Figs. 4 and 5. The hard cations show a pronounced affinity for coordination with the harder ligands while soft cations prefer coordination with softer ligands [15]. In MMTDMF ambidentate SCN^- ions are S-bonded to Hg(II) and N-bonded to Mn(II) ions (Fig. 4). This coordination polymer is composed of a three dimensional network because of the –Hg–S–C≡N–Mn– bridge. This relatively strong metal-ligand bond gives good stability. Hg(II) exhibits a distorted tetrahedral structure while Mn(II) is octahedrally coordinated to four 'N' atoms and two O(DMF) atoms. The DMF coordinates to Mn(II) through its carbonyl O atom forming a distorted polyhedron. The crystal data and structure refinement are given in Table 2. The selected bond lengths (Å) and angles (°) are listed in Table 3. The atomic coordinates and equivalent isotropic displacement parameters are given in Table 4. The Mn(I)–O(1) bond distance [2.250(3) Å] and Mn(1)–O(1)–Mn(1) bond angle [103.24(11)°] are comparable to that observed for $MnHg(SCN)_4$(DMSO) complex [16]. The Mn–N bond lengths vary with respect to orientation (2.157–2.197 Å) and the longest distance is for Mn–O(DMF) (2.241 Å). Dissimilarities are quite likely due to DMF coordination with MMTC through O atom. The structural features are fundamentally the same as that of DMSO complex of $MnHg(SCN)_4$ [16] (Table 5). The S–C bond lengths in MMTDMF (1.649–1.660 Å; mean 1.6522 Å) are considerably shorter than the typical single S–C bond length of 1.81 Å. In $MnHg(SCN)_4$ also S–C bond length is ~1.659 Å.

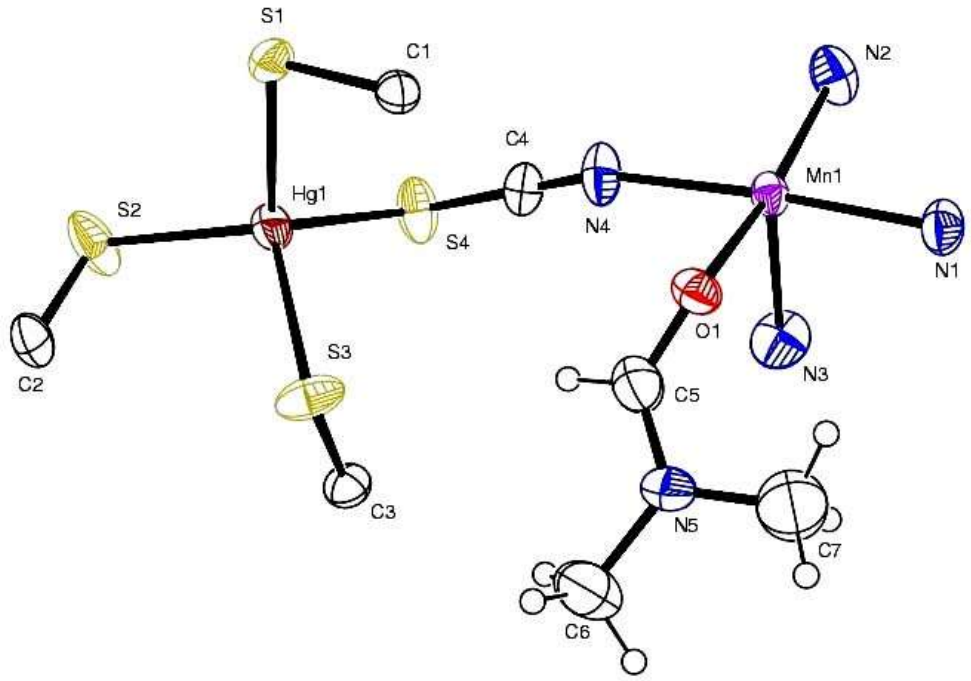

Fig. 4 ORTEP drawing of a part of polymeric complex with adopted atom numbering scheme (hydrogen atoms are shown as small circles with arbitrary radii)

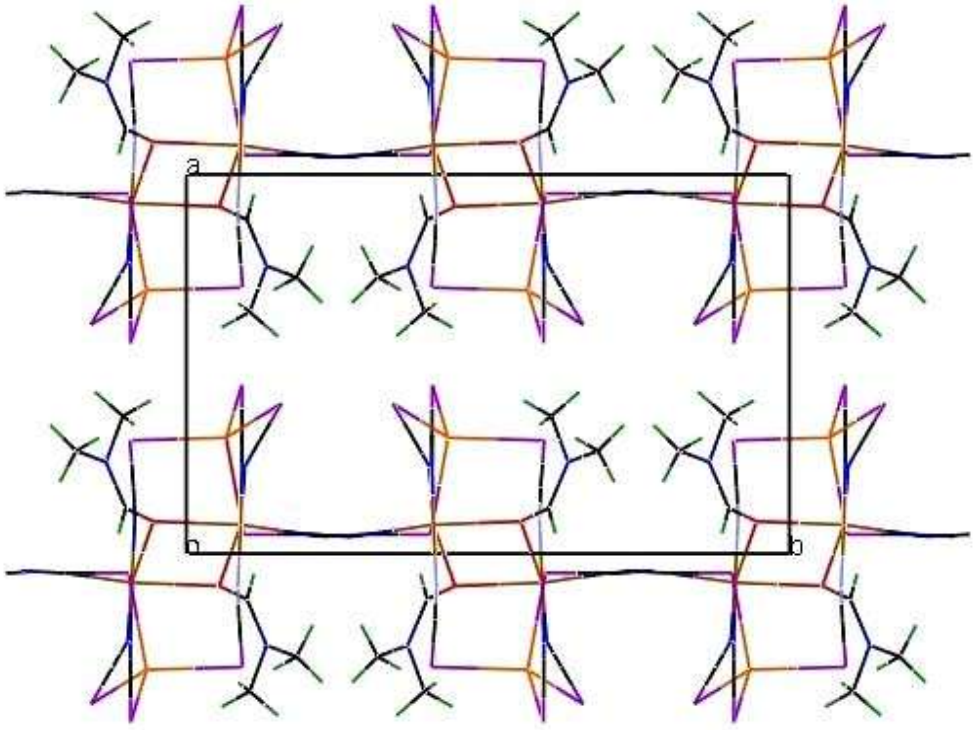

Fig. 5 Packing diagram of $MnHg(SCN)_4(C_3H_7NO)$

A close observation of bond parameters of MMTDMF reveals that they are comparable to that of MMTC. Considerable difference is observed for Mn–N bond length. It could be due to the change of geometry from tetrahedral in MMTC to octahedral in MMTDMF. MnN_4 tetrahedron in MMTC changes to MnN_4O_2 octahedron in MMTDMF structure due to the coordination of bimetallic thiocyanate with DMF through O atoms. The coordination geometry around the manganese atoms in DMF complex is distorted octahedron while it is distorted tetrahedron in $MnHg(SCN)_4$. The angle of N(4)–Mn(1)–N(1) is 175.66(17)°, clearly showing the effective linearity. The S–Hg–S angle is 110.88° (mean) which indicates the tetrahedral environment around the metal ion and the distortion with respect to idealized tetrahedral geometry in coordination angle.

Table 2 Crystal data and structure refinement for MMTDMF

Empirical formula	$C_7H_7HgMnN_5OS_4$	Reflections collected/unique	26394/7380 [R_{int} = 0.0601]
Formula weight	560.95	Completeness to theta = 25.00	100.0 %
Temperature	293(2) K	Absorption correction	Semi-empirical from

			equivalents
Wavelength	0.71073 Å	Max. and min. transmission	0.2280 and 0.1449
Crystal system, space group	Monoclinic, $P2_1/c$	Refinement method	Full-matrix least-squares on F^2
Unit cell dimensions	a = 9.9602(3) Å, α = 90° b = 15.5228(5) Å, β = 104.0630(10) c = 11.0710(3) Å, γ = 90°	Data/restraints/parameters	7380/1/176
Volume	1660.39(9) $Å^3$	Goodness-of-fit on F^2	1.016
Z, Calculated density	4, 2.244 Mg/m^3	Final R indices [$I > 2\sigma(I)$]	R_1 = 0.0395, wR_2 = 0.0870
Absorption coefficient	10.495 mm^{-1}	R indices (all data)	R_1 = 0.0807, wR_2 = 0.0963
F(000)	1044	Extinction coefficient	0.0057(2)
Crystal size	0.30 × 0.20 × 0.20 mm	Largest diff. peak and hole	2.679 and –1.263 $e.A^{-3}$
θ range for data collection	2.31 to 35.59°	CCDCC data deposition number	676706
Limiting indices	–16<=h<=15, –25<=k<=22, –17<=l<=17		

Table 3 Bond lengths [Å] and angles [°] for MMTDMF

Bond length		S(1)–Hg(1)	2.5501(11)	C(5)–N(5)–C(6)	119.7(4)
C(1)–N(1)#1	1.135(5)	S(2)–Hg(1)	2.4917(12)	C(7)–N(5)–C(6)	121.7(8)
C(1)–S(1)	1.660(4)	S(3)–Hg(1)	2.5384(11)	C(7')–N(5)–C(6)	112.9(7)
C(2)–N(2)#2	1.134(6)	S(4)–Hg(1)	2.5171(12)	C(5)–O(1)–Mn(1)	124.7(3)
C(2)–S(2)	1.655(5)	Mn(1)–O(1)#1	2.250(3)	C(5)–O(1)–Mn(1)#1	124.7(3)
C(3)–N(3)#3	1.120(6)	**Bond angle**		Mn(1)–O(1)–Mn(1)#1	103.24(11)
C(3)–S(3)	1.645(4)	N(1)#–C(1)–S(1)	178.5(4)	C(1)–S(1)–Hg(1)	97.53(14)
C(4)–N(4)	1.143(5)	N(2)#2–C(2)–S(2)	175.9(4)	C(2)–S(2)–Hg(1)	98.62(15)
C(4)–S(4)	1.649(4)	N(3)#3–C(3)–S(3)	176.9(4)	C(3)–S(3)–Hg(1)	99.78(15)
C(5)–O(1)	1.256(6)	N(4)–C(4)–S(4)	178.4(4)	C(4)–S(4)–Hg(1)	98.60(16)
C(5)–N(5)	1.291(6)	O(1)–C(5)–N(5)	125.0(5)	N(3)–Mn(1)–N(2)	99.86(18)
C(5)–H(5)	0.9300	O(1)–C(5)–H(5)	117.5	N(3)–Mn(1)–N(1)	91.05(16)
C(6)–N(5)	1.474(6)	N(5)–C(5)–H(5)	117.5	N(2)–Mn(1)–N(1)	92.30(16)
C(6)–H(6A)	0.9600	N(5)–C(6)–H(6A)	109.5	N(3)–Mn(1)–N(4)	87.38(17)
C(6)–H(6B)	0.9600	N(5)–C(6)–H(6B)	109.5	N(2)–Mn(1)–N(4)	91.96(17)
C(6)–H(6C)	0.9600	H(6A)–C(6)–H(6B)	109.5	N(1)–Mn(1)–N(4)	175.66(17)
C(7')–N(5)	1.413(14)	N(5)–C(6)–H(6C)	109.5	N(3)–Mn(1)–O(1)	93.50(15)
C(7')–H(7'1)	0.9600	H(6A)–C(6)–H(6C)	109.5	N(2)–Mn(1)–O(1)	166.62(15)
C(7')–H(7'2)	0.9600	H(6B)–C(6)–H(6C)	109.5	N(1)–Mn(1)–O(1)	86.70(14)
C(7')–H(7'3)	0.9600	N(5)–C(7')–H(7'1)	109.5	N(4)–Mn(1)–O(1)	89.36(14)
C(7)–N(5)	1.399(14)	N(5)–C(7')–H(7'2)	109.5	N(3)–Mn(1)–O(1)#1	170.13(15)
C(7)–H(71)	0.9600	N(5)–C(7')–H(7'3)	109.5	N(2)–Mn(1)–O(1)#1	89.91(15)
C(7)–H(72)	0.9600	N(5)–C(7)–H(71)	109.5	N(1)–Mn(1)–O(1)#1	90.01(13)
C(7)–H(73)	0.9600	N(5)–C(7)–H(72)	109.5	N(4)–Mn(1)–O(1)#1	90.85(15)
N(1)–C(1)#1	1.135(5)	H(71)–C(7)–H(72)	109.5	O(1)–Mn(1)–O(1)#1	76.76(11)
N(1)–Mn(1)	2.190(4)	H(72)–C(7)–H(73)	109.5	S(2)–Hg(1)–S(4)	109.53(5)
N(2)–C(2)#4	1.134(6)	C(1)#1–N(1)–Mn(1)	176.2(4)	S(2)–Hg(1)–S(3)	111.80(5)
N(2)–Mn(1)	2.173(4)	C(2)#4–N(2)–Mn(1)	178.4(4)	S(4)–Hg(1)–S(3)	110.43(4)
N(3)–C(3)#5	1.120(6)	C(3)#5–N(3)–Mn(1)	168.3(4)	S(2)–Hg(1)–S(1)	111.76(5)
N(3)–Mn(1)	2.157(4)	C(4)–N(4)–Mn(1)	162.7(4)	S(4)–Hg(1)–S(1)	112.53(4)
N(4)–Mn(1)	2.197(4)	C(5)–N(5)–C(7)	115.6(8)	S(3)–Hg(1)–S(1)	100.57(4)
O(1)–Mn(1)	2.241(3)	C(5)–N(5)–C(7')	124.7(7)		
O(1)–Mn(1)#1	2.250(3)	C(7)–N(5)–C(7')	35.1(8)		

Table 4 Atomic coordinates (× 10^4) and equivalent isotropic displacement parameters (A^2 × 10^3) for MMTDMF. U (eq) is defined as one third of the trace of the orthogonalized U_{ij} tensor

Atom	**X**	**Y**	**Z**	**U (eq)**
C(1)	1742(4)	–875(3)	8132(4)	36(1)
C(2)	3177(5)	926(3)	12884(4)	46(1)
C(3)	509(4)	2013(3)	9721(4)	39(1)
C(4)	2976(4)	1214(3)	7192(4)	41(1)
C(5)	–1199(5)	1005(4)	6290(5)	56(1)

C(6)	–2712(7)	1826(4)	7226(6)	76(2)
C(7)	–3627(15)	1051(11)	5322(14)	82(3)
C(7)	–3223(17)	1419(14)	4967(14)	82(3)
N(1)	–893(4)	853(2)	2762(3)	45(1)
N(2)	2362(5)	927(3)	3442(4)	55(1)
N(3)	450(5)	2268(3)	4651(4)	60(1)
N(4)	2303(4)	972(3)	6267(3)	53(1)
N(5)	–2415(4)	1331(2)	6185(4)	46(1)
O(1)	–851(3)	545(2)	5484(3)	39(1)
S(1)	2986(1)	–934(1)	9435(1)	40(1)
S(2)	4452(1)	922(10	12165(1)	71(1)
S(3)	505(1)	954(1)	9789(1)	52(1)
S(4)	3967(1)	1582(1)	8506(1)	56(1)
Mn(1)	763(1)	903(1)	4473(1)	32(1)
Hg(1)	3059(1)	660(1)	10002(1)	42(1)

Table 5 Comparison of the bond parameters of MMTC and MMTDMF

Parameters	**MMTC [14]**	**MMTDMF**
S–C (Å)	1.659(8)	1.6522(5)
C–N (Å)	1.140(14)	1.1330(4)
Mn–N (Å)	2.070(13)	2.1792(4)
Hg–S (Å)	2.565(2)	2.5243(12)
S–C–N(°)	178(1)	~ 178

3.4. Optical transmittance spectroscopy

The UV transparency cut off of MMTC occurs at 385 nm while that of MMTDMF crystal occurs at 366 nm (Fig. 6). The coordination complex possesses shorter cut off wavelength and shows hypsochromic shift compared with MMTC. The transparent nature in UV–Vis–NIR region can be exploited for many NLO applications [6].

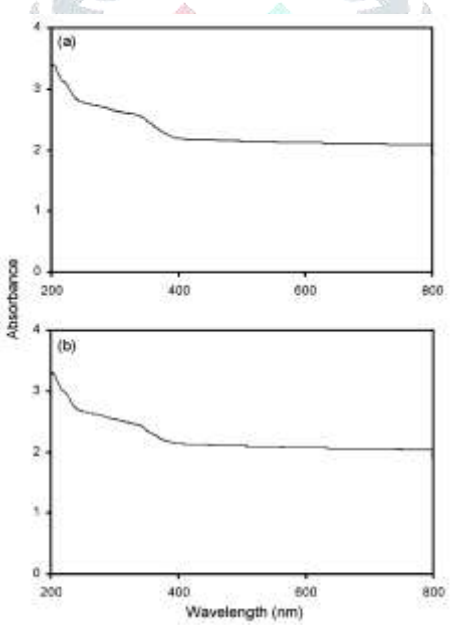

Fig. 6 UV-Vis spectra of (a) MMTC and (b) MMTDMF

3.5. SEM and EDS

SEM investigation reveals the formation of structure defect centers in MMTC (Fig. 7a) while MMTDMF exhibits rod shaped microcrystalline structures (Figs. 7b and 7c). The presence of Mn and Hg in MMTDMF is confirmed by EDS (Fig. 8).

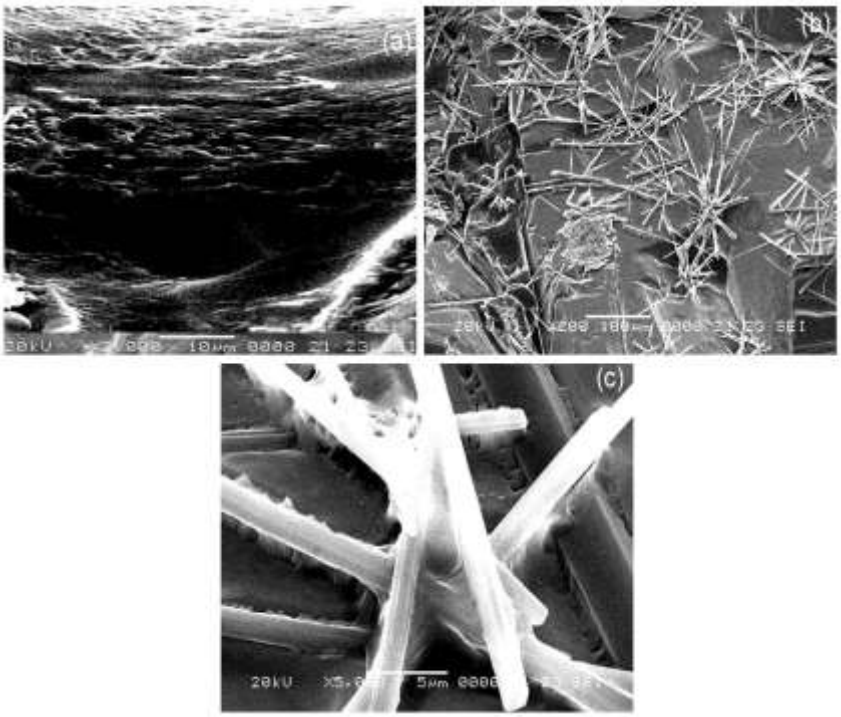

Fig. 7 SEM micrographs of (a) MMTC, (b) MMTDMF (× 200) and (c) MMTDMF (× 5000)

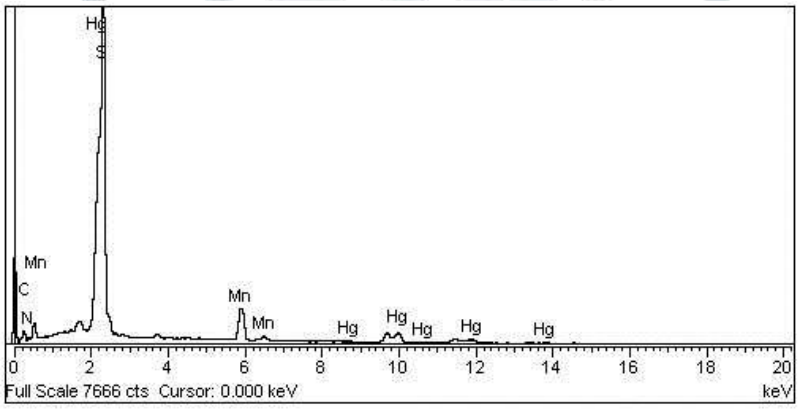

Fig. 8 EDS spectrum of MMTDMF

3.6. Second harmonic generation (SHG)

Intensity of SHG gives an indication of NLO efficiency of the material. Input radiation was 1.35 mJ/pulse and microcrystalline KDP is used for comparison. SHG output of MMTC and its DMF coordination polymer are given in Table 6.

Table 6 Comparison of the bond parameters of MMTC and MMTDMF

Parameters	MMTC [14]	MMTDMF
S–C (Å)	1.659(8)	1.6522(5)
C–N (Å)	1.140(14)	1.1330(4)
Mn–N (Å)	2.070(13)	2.1792(4)
Hg–S (Å)	2.565(2)	2.5243(12)
S–C–N(°)	178(1)	~ 178

MMTC possesses a very high nonlinearity [14]. DMF coordination polymer of MMTC is almost NLO inactive (Table 6) and it is not surprising since the MMTDMF belongs to monoclinic system with the space group (centrosymmetric) $P2_1/c$. It appears that the coordination with DMF destroys the noncentrosymmetry of MMTC leading centrosymmetry. Interestingly, DMSO complex of $CdHg(SCN)_4$ exhibits the largest second harmonic intensity [17]. It is obvious that the nature of the ligand determines the NLO activities of bimetallic thiocyanato complexes. It has been reported that the high nonlinearity of $[ZnCd(SCN)_4]$ [18] and MMTC [14] is attributed to structural factors. The effective charge transfer through the charge transfer bridge –S–C≡N– and the effective sum of microscopic hyperpolarizabilities result in high NLO activity. In the present investigations, the NLO inactivity of MMTDMF could be due to cancellation effects of hyperpolarizabilites and ineffective charge transfer through bridging ligand due to structural aspects. As observed in DAST studies [4], the structural modifications of MMTC because of coordination with DMF affect the NLO activity and make it inactive.

Even though the NLO activity of MMTDMF is negligible, the paramagnetic behaviour of Mn(II) and the possibility of Mn(II) → Mn(III) resulting in electrooptic effect and enhanced photoconductivity effect make this complex a promising useful material. These aspects need further probe. Also, the complex is expected to exhibit weak antiferromagnetism as reported previously in the case of DMSO complex of $MnHg(SCN)_4$ [17].

4. CONCLUSION

The coordination geometry of the central Mn(II) atom is distorted octahedron while that of Hg(II) is distorted tetrahedron in MMTDMF coordination polymers. The main conclusion of the study is, structural modifications of bimetallic thiocyanate complex, $AB(SCN)_4$ by coordination with DMF ligand disturb the nonlinearity. In the present investigation, the polymer crystallizes in a centrosymmetric space group, leading to NLO inactivity.

5. SUPPLEMENTARY MATERIAL

CCDC 676706 contains the supplementary crystallographic data for this paper. These data can be obtained free of charge via www.ccdc.cam.ac.uk/const/retrieving.html (or from the Cambridge Crystallographic Data Centre, 12, Union Road, Cambridge CB2 1EZ, UK; fax: +44 1223 336033; e-mail: deposit@ccdc.cam.ac.uk).

REFERENCES

[1] Gunasekaran, S. and Ponnusamy, S. 2006. Growth and characterization of cadmium magnesium tetra thiocyanate crystals. Crystal Research and Technology, 41: 130–137.

[2] Duan, X.L., Yuan, D.R., Wang, X.Q., Cheng, X.F., Yang, Z.H., Guo, S.Y., Sun, H.Q., Xu, D. and Lu, M.K. 2002. Preparation and characterization of nonlinear optical crystal materials: cadmium mercury thiocyanate and its Lewis basis adducts. Crystal Research and Technology, 37: 446–455.

[3] Kityk, I.V. 1991. Band energy structure calculations in semiconductors. Physics of the Solid State, 33: 1026–1030.

[4] Yang, Z., Worle, M., Mutter, L., Jazbinesk, M. and Gunter, P. 2007. Synthesis, crystal structure, and second-order nonlinear optical properties of new stilbazolium salts. Crystal Growth and Design, 7: 83–86.

[5] Wang, X.Q., Xu, D., Lu, M.K., Yuan, D.R. and Xu, S.X. 2001. Crystal growth and characterization of the organometallic nonlinear optical crystal: manganese mercury thiocyanate (MMTC). Materials Research Bulletin, 36: 879–887.

[6] Joseph, G.P., Philip, J., Rajarajan, K., Rajasekar, S.A., Arul Pragasam A.J., Thamizharasan, K., Ravikumar, S.M. and Sagayaraj, P. 2006. Growth and characterization of an organometallic nonlinear optical crystal of manganese mercury thiocyanate (MMTC). Journal of Crystal Growth, 296: 51–57.

[7] Wang, X.Q., Yu, W.T., Lu, D.U.M.K., Yuan, D.R. and Lu, G.T. 2000. Manganese mercury thiocyanate (MMTC) glycol monomethyl ether. Acta Crystallographica C, 56: 647–648.

[8] Kurtz, S.K. and Perry, T.T. 1968. A powder technique for the evaluation of nonlinear optical materials. Journal of Applied Physics, 39: 3798–3813.

[9] Nakamoto, K. 1978. Infrared and Raman spectra of inorganic and coordination compounds. 3rd ed., John Wiley and Sons, New York.

[10] Silverstein, R.M. and Webster, F.X. 1998. Spectroscopic identification of organic compounds. 6th ed., John Wiley and Sons, New York.

[11] Spectral Database for Organic Compounds, AIST, Japan.

[12] Martinez-Lillo, J., Armentanao, D., Munno, G.D., Lloret, F., Julve, M. and Faus, J. 2006. Rhenium(IV) cyanate complexes: Synthesis, crystal structures and magnetic properties of $NBu_4[ReBr_4(OCN)(DMF)]$ and $(NBu_4)_2[ReBr(OCN)_2(NCO)_3]$. Inorganica Chimica Acta, 359: 4343–4349.

[13] Yatsimirskii, K.B. 1977. Spectroscopic studies on coordination compounds formed in molten salts. Pure and Applied Chemistry, 49: 115–124.

[14] Yan, Y.X., Fang, Q., Yuan, D.R., Tian, Y.P., Liu, Z., Wang, X.M., Jiang, M.H., Williams, D., Siu, A. and Cai, Z.G. 1999. Synthesis, structure and non-linear optical properties of manganese mercury tetrathiocyanate. Chinese Chemical Letters, 10: 257–260.

[15] Balarew, C. and Duhlev, R. 1984. Application of the hard and soft acids and bases concept to explain ligand coordination in double salt structures. Journal of Solid State Chemistry, 55: 1–6.

[16] Li, C.S., Xue, L., Che, Y.X., Luo, F., Zheng, J.M. and Mak, T.C.W. 2007. Synthesis, structure and magnetic properties of two μ-oxo and thiocyanato-bridged manganese(II)-mercury(II) coordination polymers. Inorganica Chimica Acta, 360: 3569–3574.

[17] Guo, S., Xu, D., Lu, M., Yuan, D., Yang, Z., Zhang, G., Sun, S., Wang, X., Zhou, M., Jiang, M., Yang, P. and Yu, W. 2000. A novel organometallic nonlinear optical complex crystal: Cadmium mercury thiocyanate dimethyl-sulphoxide. Progress in Crystal Growth and Characterization of Materials, 40: 111–114.

[18] Joseph, G.P., Rajarajan, K., Vimalan, M., Thomas, P.C., Madhavan, J., Ravikumar, S.M., Mohamed, M.G., Mani, G. and Sagayaraj, P. 2007. Growth and characterization of non-linear optical crystal $ZnCd(SCN)_4$. Crystal Research and Technology, 42: 247–252.